AD

US ARMY MATERIEL COMMAND

MEMORANDUM REPORT BRL-MR-3518

STRESS MEASUREMENTS IN GLASS DURING SHAPED-CHARGE JET PENETRATIONS

Robert E. Franz
William Lawrence

May 1986

US ARMY BALLISTIC RESEARCH LABORATORY
ABERDEEN PROVING GROUND, MARYLAND

DISCLAIMER NOTICE

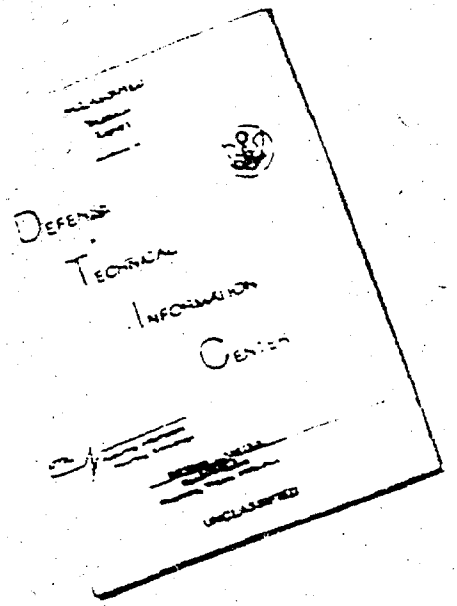

THIS DOCUMENT IS BEST QUALITY AVAILABLE. THE COPY FURNISHED TO DTIC CONTAINED A SIGNIFICANT NUMBER OF PAGES WHICH DO NOT REPRODUCE LEGIBLY.

Destroy this report when it is no longer needed.
Do not return it to the originator.

Additional copies of this report may be obtained from the National Technical Information Service, U. S. Department of Commerce, Springfield, Virginia 22161.

The findings in this report are not to be construed as an official Department of the Army position, unless so designated by other authorized documents.

The use of trade names or manufacturers' names in this report does not constitute indorsement of any commercial product.

UNCLASSIFIED

SECURITY CLASSIFICATION OF THIS PAGE *(When Data Entered)*

REPORT DOCUMENTATION PAGE		READ INSTRUCTIONS BEFORE COMPLETING FORM
1. REPORT NUMBER Memorandum Report BRL-MR-3518	2. GOVT ACCESSION NO. AD-A168 247	3. RECIPIENT'S CATALOG NUMBER
4. TITLE *(and Subtitle)* Stress Measurements in Glass During Shaped-Charge Jet Penetration		5. TYPE OF REPORT & PERIOD COVERED 6. PERFORMING ORG. REPORT NUMBER
7. AUTHOR(s) Robert E. Franz William Lawrence		8. CONTRACT OR GRANT NUMBER(s)
9. PERFORMING ORGANIZATION NAME AND ADDRESS US Army Ballistic Research Laboratory ATTN: SLCBR-TB Aberdeen Proving Ground, MD 21005-5066		10. PROGRAM ELEMENT, PROJECT, TASK AREA & WORK UNIT NUMBERS 1L161102AH43
11. CONTROLLING OFFICE NAME AND ADDRESS US Army Ballistic Research Laboratory ATTN: SLCBR-DD-T Aberdeen Proving Ground, MD 21005-5066		12. REPORT DATE May 1986 13. NUMBER OF PAGES 33
14. MONITORING AGENCY NAME & ADDRESS*(if different from Controlling Office)*		15. SECURITY CLASS. *(of this report)* UNCLASSIFIED 15a. DECLASSIFICATION/DOWNGRADING SCHEDULE

16. DISTRIBUTION STATEMENT *(of this Report)*

Approved for public release, distribution unlimited.

17. DISTRIBUTION STATEMENT *(of the abstract entered in Block 20, if different from Report)*

18. SUPPLEMENTARY NOTES

19. KEY WORDS *(Continue on reverse side if necessary and identify by block number)*

Shaped-charge jet	Fracture velocity
Penetration velocity	Constantan gage
Manganin gage	Glass targets

20. ABSTRACT *(Continue on reverse side if necessary and identify by block number)*

Stresses were measured in glass targets in the vicinity of a penetrating shaped-charge jet. Stress levels of approximately 0.3 gigapascals were measured 12-20 mm away from a jet formed by a 35 mm copper liner. High speed framing camera photographs showed that the penetration velocity in the glass was 2.57 km/s and the glass fracture velocity was 2.10 km/s.

DD FORM 1 JAN 73 1473 EDITION OF 1 NOV 65 IS OBSOLETE

UNCLASSIFIED

SECURITY CLASSIFICATION OF THIS PAGE *(When Data Entered)*

TABLE OF CONTENTS

		Page
	LIST OF ILLUSTRATIONS.	5
I.	INTRODUCTION	7
II.	EXPERIMENTAL PROCEDURE	7
III.	RESULTS.	11
IV.	DISCUSSION	16
V.	CONCLUSIONS.	27
	REFERENCES	29
	DISTRIBUTION LIST.	31

LIST OF ILLUSTRATIONS

FIG. NO.		Page
1	Shaped Charge Used in Penetration Experiments.	8
2	Perpendicular-Layer Glass Target	9
3	Parallel-Layer Glass Target.	10
4	Gage Placement in Shallow Slot	12
5	Manganin Grid Gage Factor	15
6	Stress Measurement from Test No. 4	17
7	Stress Measurement from Test No. 5	18
8	Stress Measurement from Test No. 8	19
9	Stress Measurement from Gage at 120.65 mm in Test No. 10 . . .	20
10	Stress Measurement from Gage at 63.5 mm in Test No. 14	21
11	Stress Measurement from Gage at 44.45 mm in Test No. 15. . . .	22
12	Stress Measurement from Gage at 63.5 mm in Test No. 15. Gage was not in slot	23
13	Stress Measurement from Test No. 16. Gage was not in slot . .	24
14	Framing Camera Frames from Test No. 8. Time between frames is 2 microseconds. The dark part of the gage slot is 16 mm wide	25
15	Framing Camera Frames from Test No. 10. Time between frames is 1.33 microseconds. Fiducial marks are spaced 25 mm apart .	26

I. INTRODUCTION

It has been known for over 40 years that glass targets are unusually effective in stopping shaped-charge jets. Studies of this effectiveness were made during and after World War II.[1] These studies established the principles of defense against shaped-charge jets using glass. Nevertheless, little is known about the physics and chemistry associated with the penetration process in glass.

This report describes some experiments made to measure dynamic stresses in glass in the vicinity of a penetrating jet. Strain-compensated stress gages and simultaneous high-speed framing camera photographs were used for this purpose. These experiments are part of a larger effort to understand the fundamentals of the jet penetration process in glass and glass-like materials.[2] The overall work also includes the use of flash radiography to observe the on-going penetration, and target recovery to observe the material after penetration.

II. EXPERIMENTAL PROCEDURE

The shaped-charge jets used in these experiments were obtained using a 35 mm diameter conical copper liner with a wall thickness of 1.57 mm and a cone angle of 45 degrees. The explosive used was Composition B. Figure 1 is a drawing of this unconfined shaped charge. When fired at a standoff of two cone diameters the jet penetrated four cone diameters in stacked 25 mm thick rolled steel plates (Rockwell hardness B81). The jet tip velocity was 6.8 km/s.

The targets consisted of stacked layers of float glass (Density = 2500 kg/m^3). The glass layers were either 25.4 mm or 19.1 mm thick and were approximately 150 mm square. They were stacked either perpendicular to the jet path or parallel to the jet path. The layers were bonded with epoxy cement (Hysol Epoxy-Patch 608 (*)) while clamped in a press. Various cover plates were used. The cover plates were either rolled homogeneous armor (RHA) or polymethylmethacralate (PMMA), or a combination of the two of different thicknesses. Table 1 gives details of the various thicknesses, orientations and materials used in each experiment. Figures 2 and 3 show drawings of typical target configurations. The shaped charges were fired at a standoff of two cone diameters above the cover plates.

Strain-compensated stress gages (Dynasen Mod. Mn/Cn 4-50-EK (**)) were used to measure stresses during jet penetration. These gages consist of two separate interlaced foil grids encased in a polyimide plastic film. One of the grids is made of manganin and is used to measure stress. The other is made of constantan and is used to measure strain. Both grids are 5 mm square and the gages are 0.127 mm thick. The measured strain is used to correct the stress measurements. More details on how the data is reduced is given in the next section.

---

*Hysol Division, The Dexter Corporation, Olean, NY 14760
**Dynasen Inc., Goleta, CA 93017

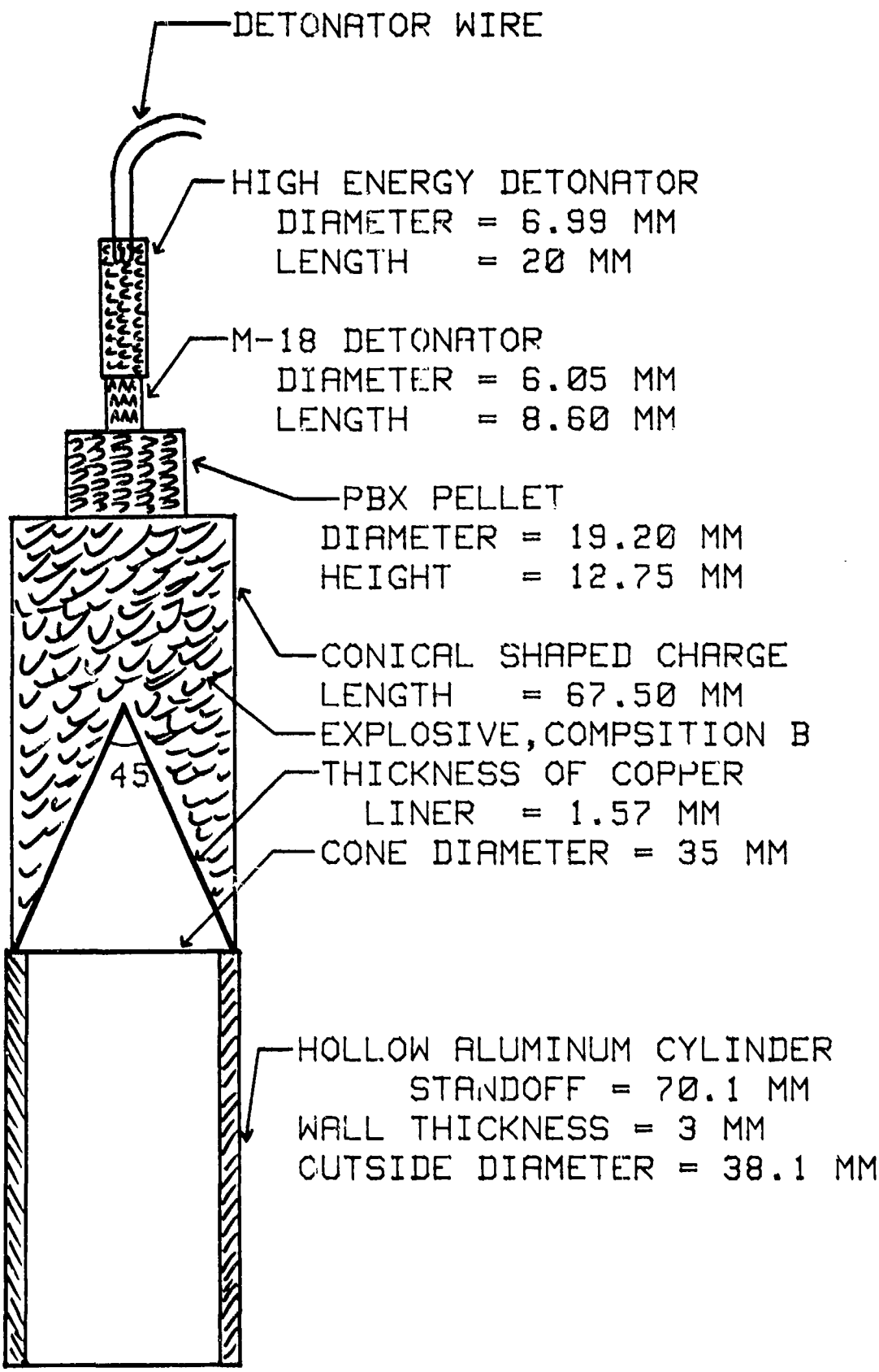

Figure 1. Shaped Charge Used in Penetration Experiments.

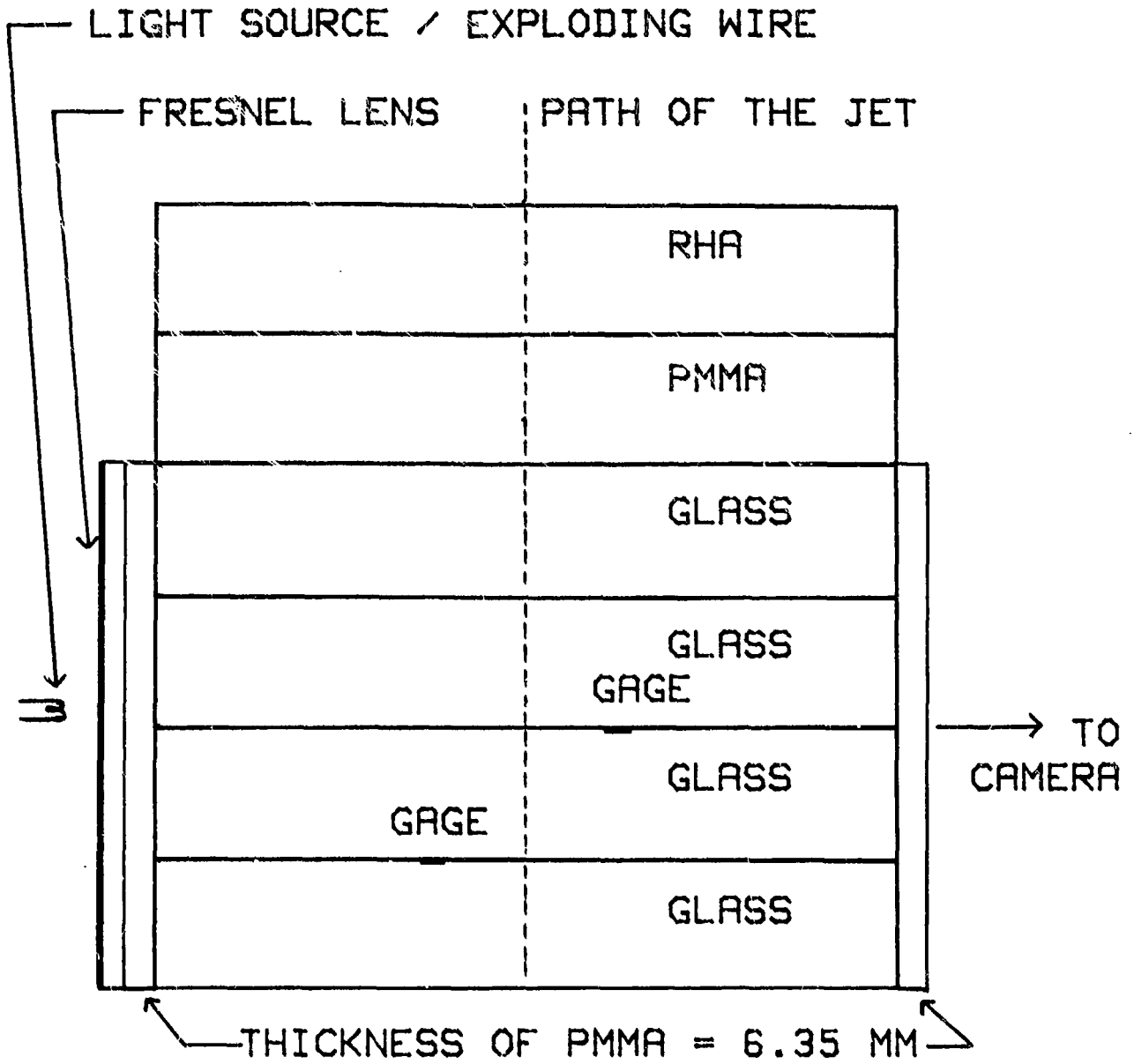

	LENGTH (MM)	WIDTH (MM)	HEIGHT/THICKNESS (MM)
GLASS	150	150	25.4
PMMA	150	150	25.4
RHA	150	150	25.4

Figure 2. Perpendicular-Layer Glass Target.

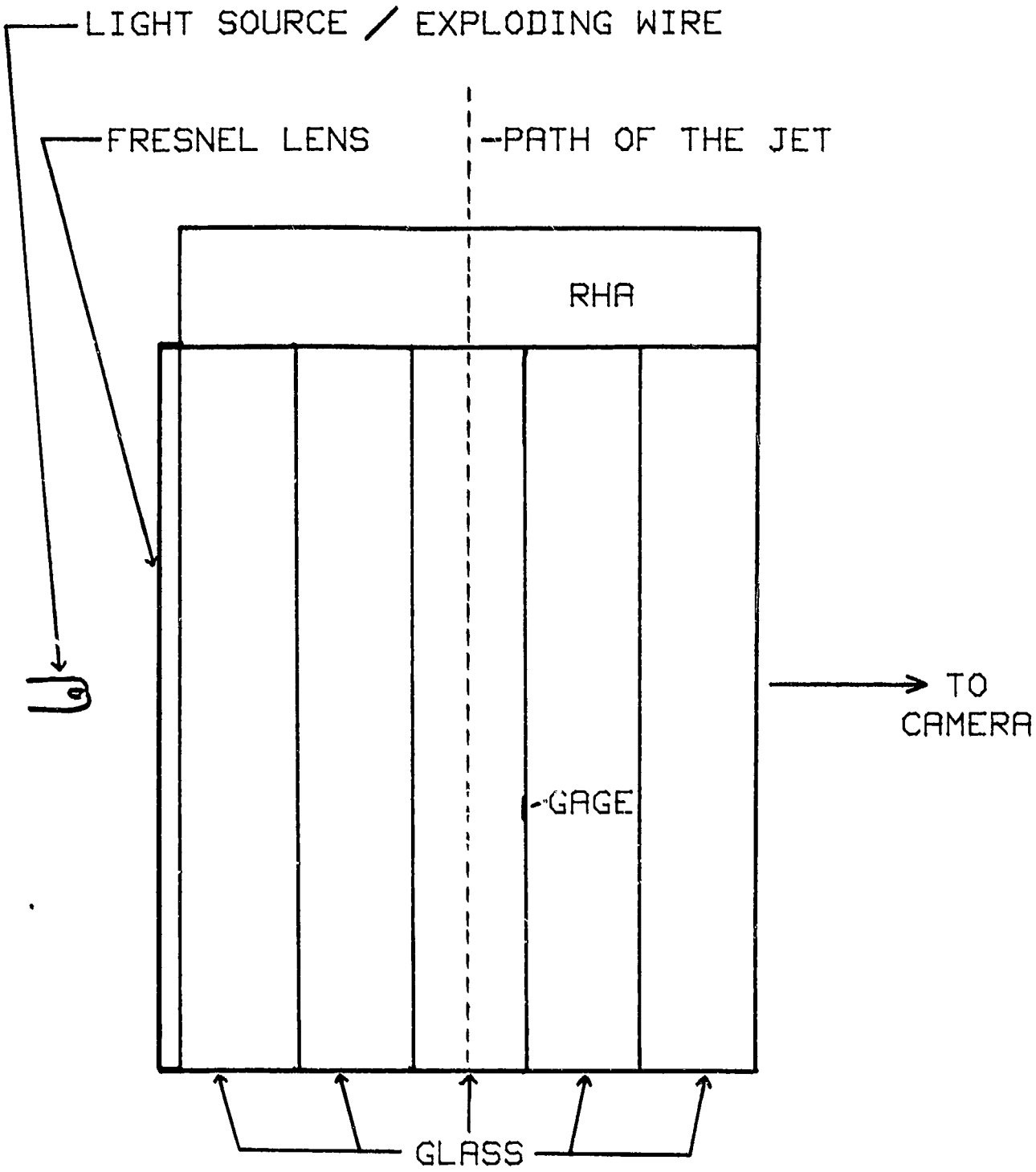

	LENGTH (MM)	WIDTH (MM)	THICKNESS (MM)
GLASS	150	127	25.4
RHA	150	127	25.4

Figure 3. Parallel-Layer Glass Target.

The gages were bonded between the layers of glass in shallow slots approximately 0.38 mm deep etched in the glass with hydrofluoric acid. The gages were placed between two layers of polytetrafluoroethylene each 0.127 mm thick to protect them from the fracturing glass. The gages and the plastic layers were bonded in the slots with the same epoxy cement used for bonding the glass layers. Figure 4 shows a drawing of the usual gage placement. The gage leads which were 95 mm long protruded from the sides of the layered targets. When the glass layers were parallel to the jet path the gage grids were also parallel. Likewise, when the layers were perpendicular the grids were perpendicular to the jet path. Table 1 also includes particulars on gage placement in each experiment. Test No. 15 and Test No. 16 were run without slots in the glass and the offset spaces caused by the thickness of the gage were filled with plastic film and epoxy cement. This was done to see if the slots affected the gage signals. Gupta and Gupta[3] have reported such disturbance in very strong materials.

The gages were attached to 93 ohm RG-62u coaxial cables which were connected to bridge circuits similar to those used by Rapacki.[4] The circuits were modified to be used with the 50 ohm Dynasen gages instead of the 120 ohm gages used by Rapacki. The signals were recorded on digital oscilloscopes (Nicolet 2090 with 204A plug-in (*)). The oscilloscopes were triggered by a circuit using a make-switch made of brass foils separated by a thin plastic film which was bonded to the front surface of the target. The impinging jet closed the switch gap circuit and triggered a delay generator that subsequently triggered the oscilloscopes.

For some of the experiments simultaneous framing camera photographs were made during jet penetration. A Cordin Model 10-010 camera was used (**). The glass targets were back-lit with an exploding tungsten wire placed near the focus of a plastic Fresnel lens. When the glass layers were parallel to the jet path, a clear optical path was perpendicular to the layers. When the layers were perpendicular to the jet path, cover plates of clear PMMA 6.35 mm thick were bonded to opposite target sides with epoxy cement to make a clear optical path for the photographs. Figures 2 and 3 show the optical setup.

III. RESULTS

The data from the two signals obtained from each gage were reduced in a manner similar to that used by Rapacki.[4] That is, calibrations were made of each circuit with known dummy gages inserted in the lines instead of the actual gage. Signals from known changes in resistance were then used to determine the circuit constants. These constants along with the known bridge and cable resistances were used to calculate the resistance of each grid at each simultaneous time step of the signals.

To calculate the stress in the glass for each time step it was assumed that the resistance of the constantan grid was not affected by the stress

---

*Nicolet Oscilloscope Division, Madison, WI 53711
**The Cordin Company, Salt Lake City, UT

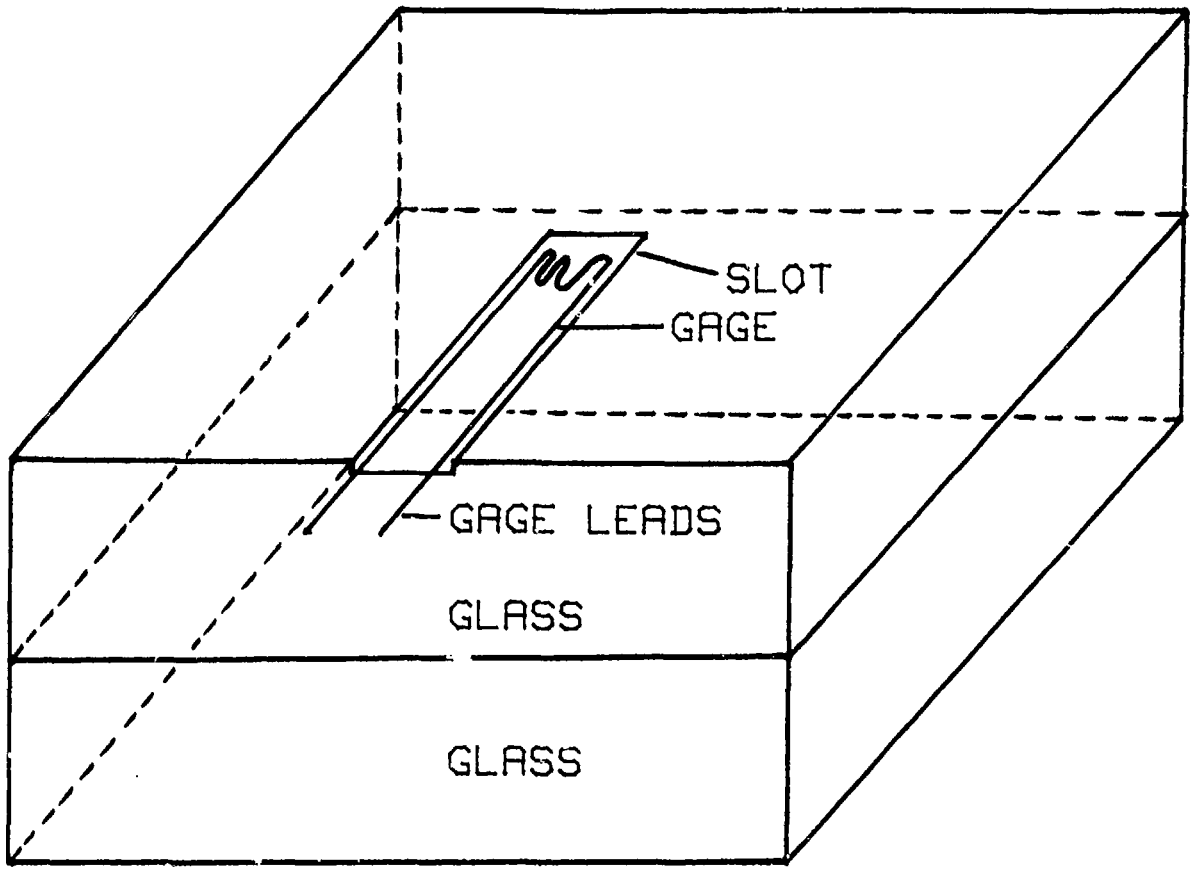

	GAGE	GLASS
LENGTH (MM)	5.0	150
WIDTH (MM)	5.0	150
THICKNESS (MM)	0.126	25.4

LENGTH OF THE GAGE LEADS = 95 MM

Figure 4. Gage Placement in Shallow Slot.

TEST NO.	GLASS PLATES		ORIENTATION OF TARGET AND GAGE TO THE INCOMING JET	GAGE IN THE SLOT		GAGE LOCATION FROM FRONT PLATE(MM)	FRONT PLATE	
	THICK (MM)	NO.		YES	NO		MATERIAL	THICK (MM)
3	25.40	5	PERPENDICULAR	YES		76.20	RHA	25.40
4	25.40	5	PARALLEL	YES		76.20	RHA	25.40
5	25.40	5	PARALLEL	YES		82.55	RHA	25.40
8	25.40	5	PARALLEL	YES		107.95	RHA/PMMA	50.80
9	25.40	4	PERPENDICULAR	YES		101.60	PMMA	50.80
				YES		127.00		
10	25.40	4	PERPENDICULAR	YES		95.25	PMMA	50.80
				YES		120 65		
14	19.05	3	PERPENDICULAR	YES		63.50	PMMA	25.40
					NO	44.45		
15	19.05	3	PERPENDICULAR	YES		44.45	PMMA	25.40
					NO	63.50		
16	25.40	4	PERPENDICULAR		NO	101.60	PMMA	50.80

STANDOFF DISTANCE BETWEEN SHAPED CHARGE AND THE FRONT PLATE = 70.10 MM

TABLE 1. TEST CONDITIONS

field that surrounded both it and the manganin grid. It was further assumed that the strain of the manganin grid was the same as in the constantan grid. Finally it was assumed that the stress in the glass was the same as that in the manganin.

The strain for each time step was calculated using the equation

$$ST = -1 + (RC/ROC)^{C.5}\ .5$$

Here

ST = strain in the constantan grid
RC = resistance of the constantan grid
ROC = the initial resistance of the constantan grid.

To calculate the stress, the resistance change associated with the strain in the manganin must first be subtracted from the total resistance change. In order to do this the strain gage factor for the manganin grid was determined from a separate static experiment. A strain-compensated stress gage was mounted on an aluminum alloy plate along with conventional strain gages (Micromeasurements EP-08-062TT-120 (*)). This plate was pulled in an universal testing machine. The data showed that the manganin grid had a gage factor of 0.7 to a strain of 0.5%. Above 0.5% strain the manganin deformed plastically and the gage factor became the same as for the constantan grid, that is, 2+ST.[5] Figure 5 is a plot of the measured apparent gage factor along with a curve calculated using a gage factor of 0.7 for the elastic strain and unloading, and a factor of 2+ST for the plastic strain. The apparent gage factor G.F., is defined as

$$G.F. = DRG/(ROG \times ST).$$

Where

DRG = the change in gage resistance,

and

ROG = the initial gage resistance.

The resistance change in the manganin due to the strain was therefore calculated by using the following equations.

For $-0.005 < ST < 0.005$

$$DRMS = 0.7 \times ST \times ROM.$$

For $ST > 0.005$

$$DRMS = (2+ST-0.005) \times (ST-0.005) \times (1+0.7\times0.005) \times ROM + (0.7\times0.005) \times ROM$$
$$= (1.995+ST) \times (ST-0.005) \times 1.0035 \times ROM + 0.0035 \times ROM$$

For $ST < -.005$

$$DRMS = (2.005+ST) \times (ST+0.005) \times 0.9965 \times ROM - 0.0035 \times ROM$$

Here

DRMS = the change in resistance of the manganin grid due to strain
ROM = the initial resistance of the manganin grid.

---

*Measurements Group, Raleigh, NC 27611

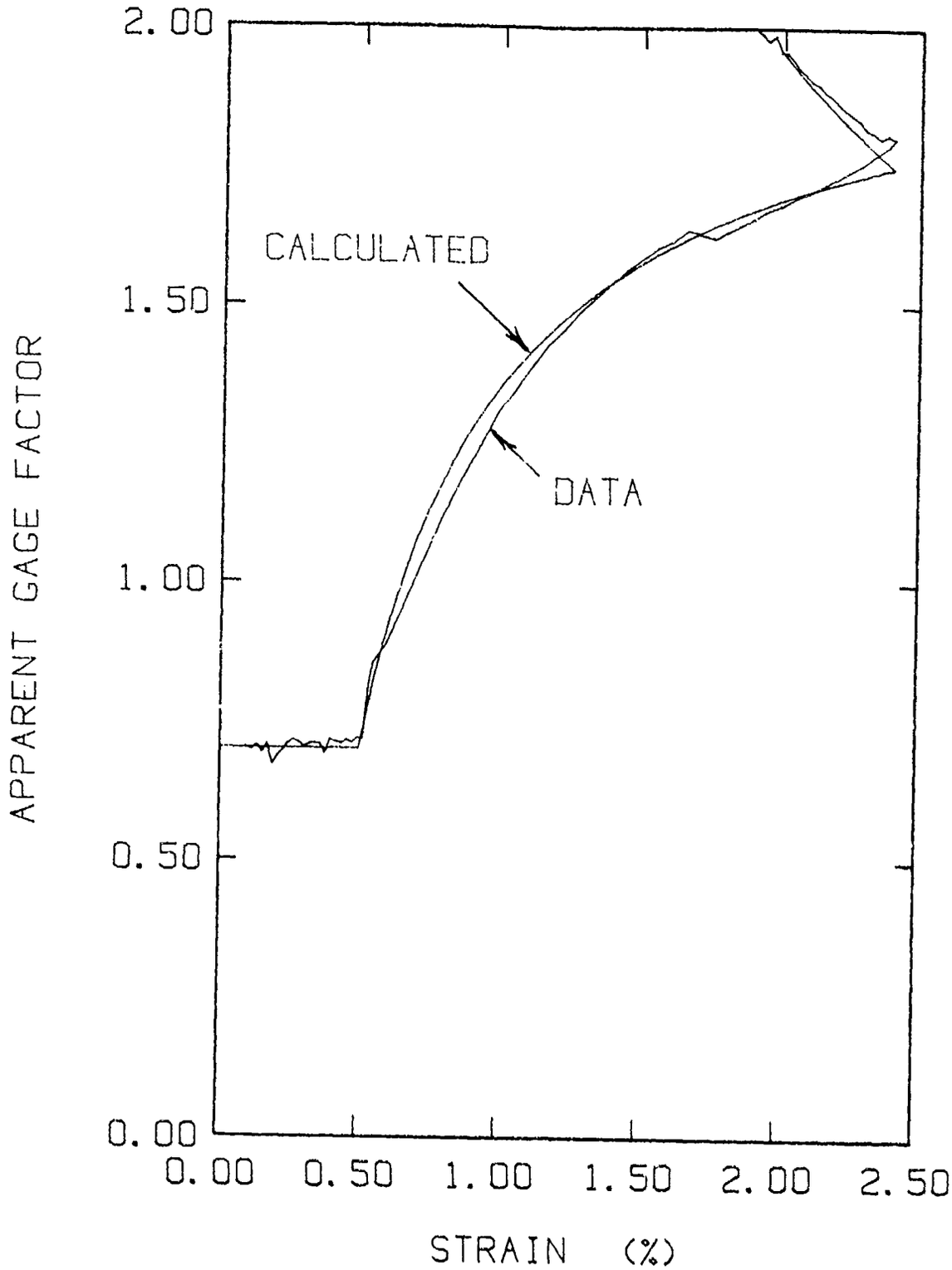

Figure 5. Manganin Grid Gage Factor

The stress in the manganin was then calculated using a cubic fit to the data of Charest.[6] This equation is

$$S = 53.19 \times (DRM/RO) - 159.91 \times (DRM/RO)^2 + 493.16 \times (DRM/RO)^3 .$$

Where

S = stress in the manganin (gigapascals)
DRM = DRMT - DRMS
RO = ROM + DRMS

and

DRMT = the total resistance change in the manganin.

Figures 6 to 13 show results obtained from this analysis. Compressive stress is positive. Figures 14 and 15 show a series of framing camera photographs. In the photographs of Figure 14 the glass layers are parallel to the jet path. There are 2 microseconds between frames. Figure 15 shows the results when the layers are perpendicular to the path. There are 1.33 microseconds between frames.

IV. DISCUSSION

The stress measurements reported here were obtained under particularly adverse physical conditions. It was learned in preliminary experiments that the foil gages and their leads had to be protected from a hostile environment which included fracturing glass. The layers of polytetraflouroethylene, used for this protection, restricted the mechanical response of the gages especially to the initial sharply rising shock waves. The response was further restricted by the electronic bandwidth of the recording equipment so that submicrosecond changes in either stress or strain could not be tracked.

The gages were approximately 19 mm to the side of the jet path for perpendicular shots and 12.7 mm from the path for parallel shots. As can be seen the stresses measured did not exceed approximately 0.3 gigapascals until the gages were on the verge of destruction from the fracturing glass. The strain in most of the shots did not contribute significantly to the stress compensation until 3 to 4 microseconds after the start of the stress signals. The usual signal showed two compressive peaks followed by either tension or compression.

Although unslotted gages did not show these distinct peaks the measured stress levels were approximately the same as for slotted gages (see Figures 12 and 13). In most cases the gages started to fail before or near jet arrival, that is, 15 to 20 microseconds after the shock arrived. For two shots the gages survived for longer times. No extremely large stresses were measured on these shots (see Figures 8 and 10). The parallel gages showed lower initial stress levels than the perpendicular gages (see Figures 6 and 8). This could result from a nonhydrodynamic stress field or from an off center jet path. These shots also had RHA cover plates which wipe off the fastest part of the jet.

The framing camera photographs clearly show that fracture occurred around the gages before the arrival of the penetrating jet. This was caused by interaction with the leading shock wave which was formed when the

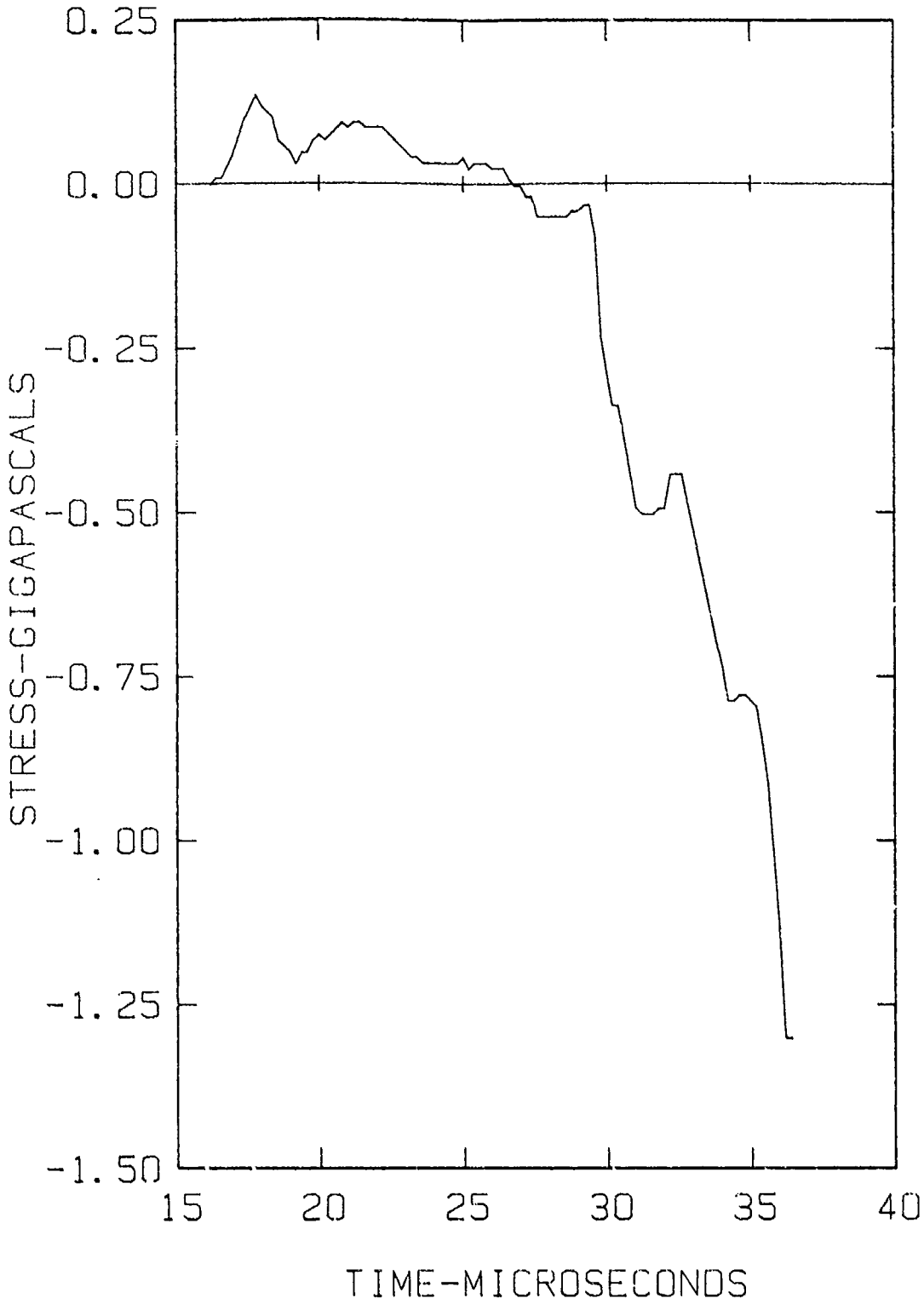

Figure 6. Stress Measurement from Test No. 4

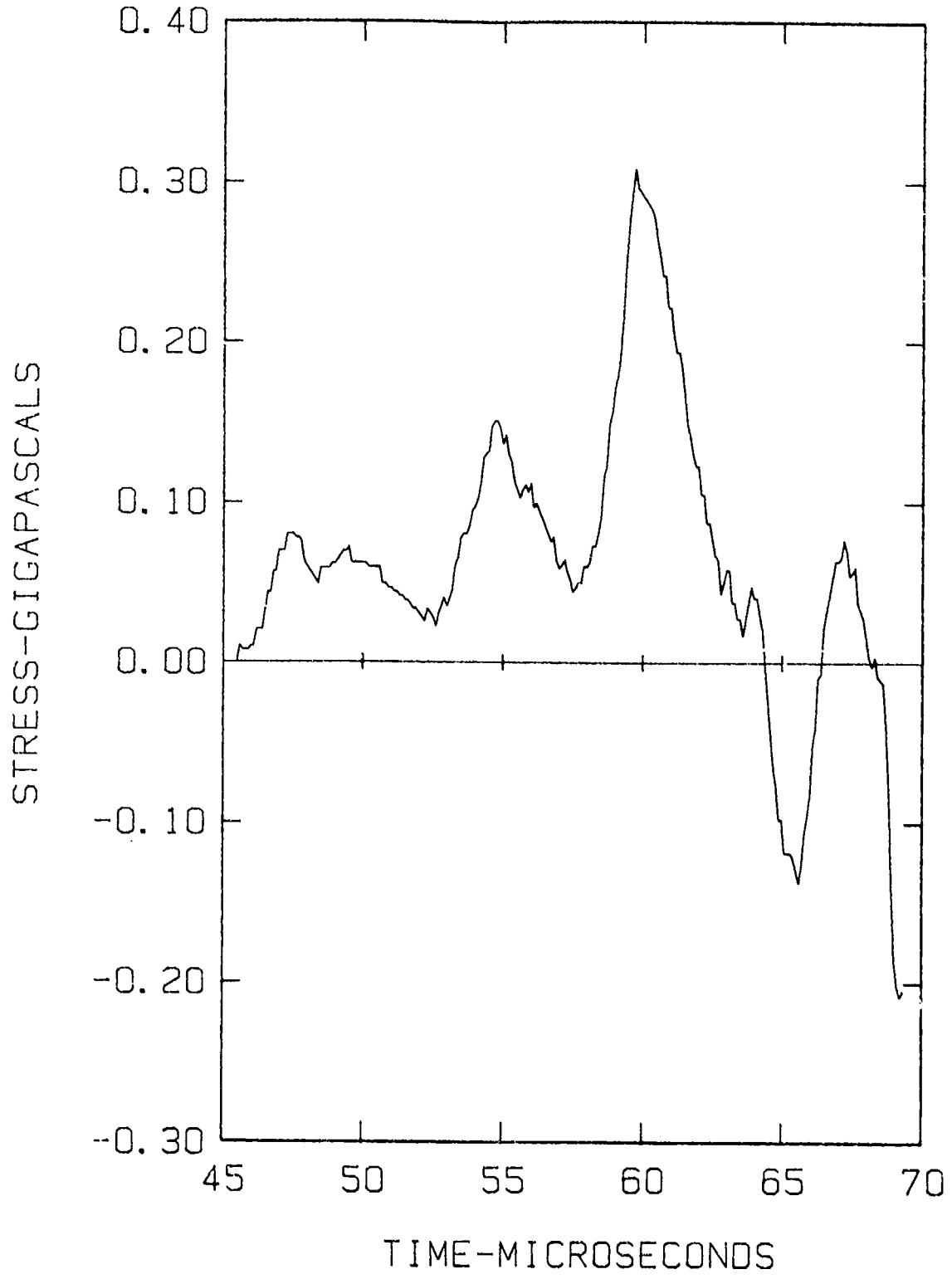

Figure 7. Stress Measurement from Test No. 5

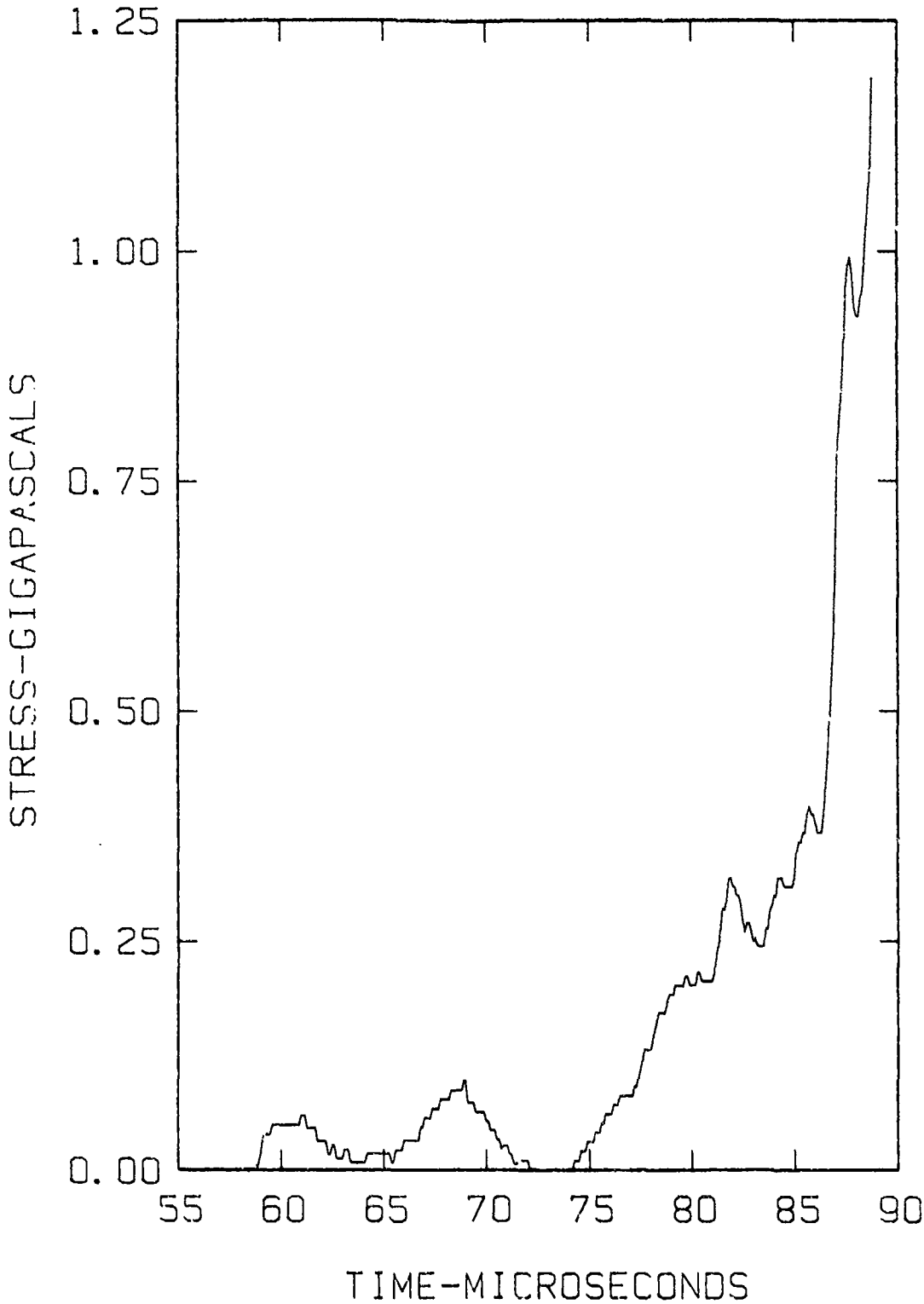

Figure 8. Stress Measurement from Test No. 8

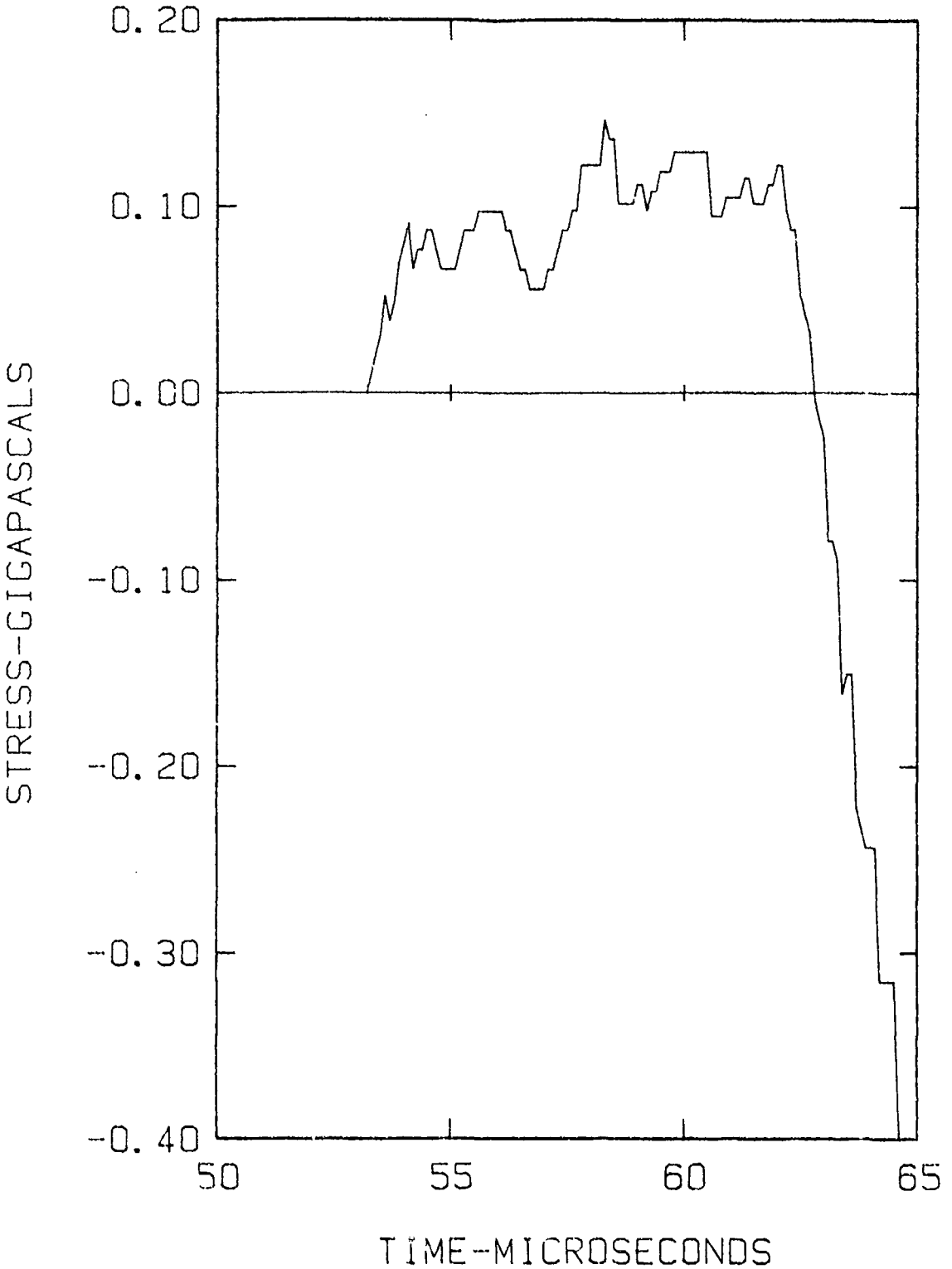

Figure 9. Stress Measurement from Gage at 120.65 mm in Test No. 10

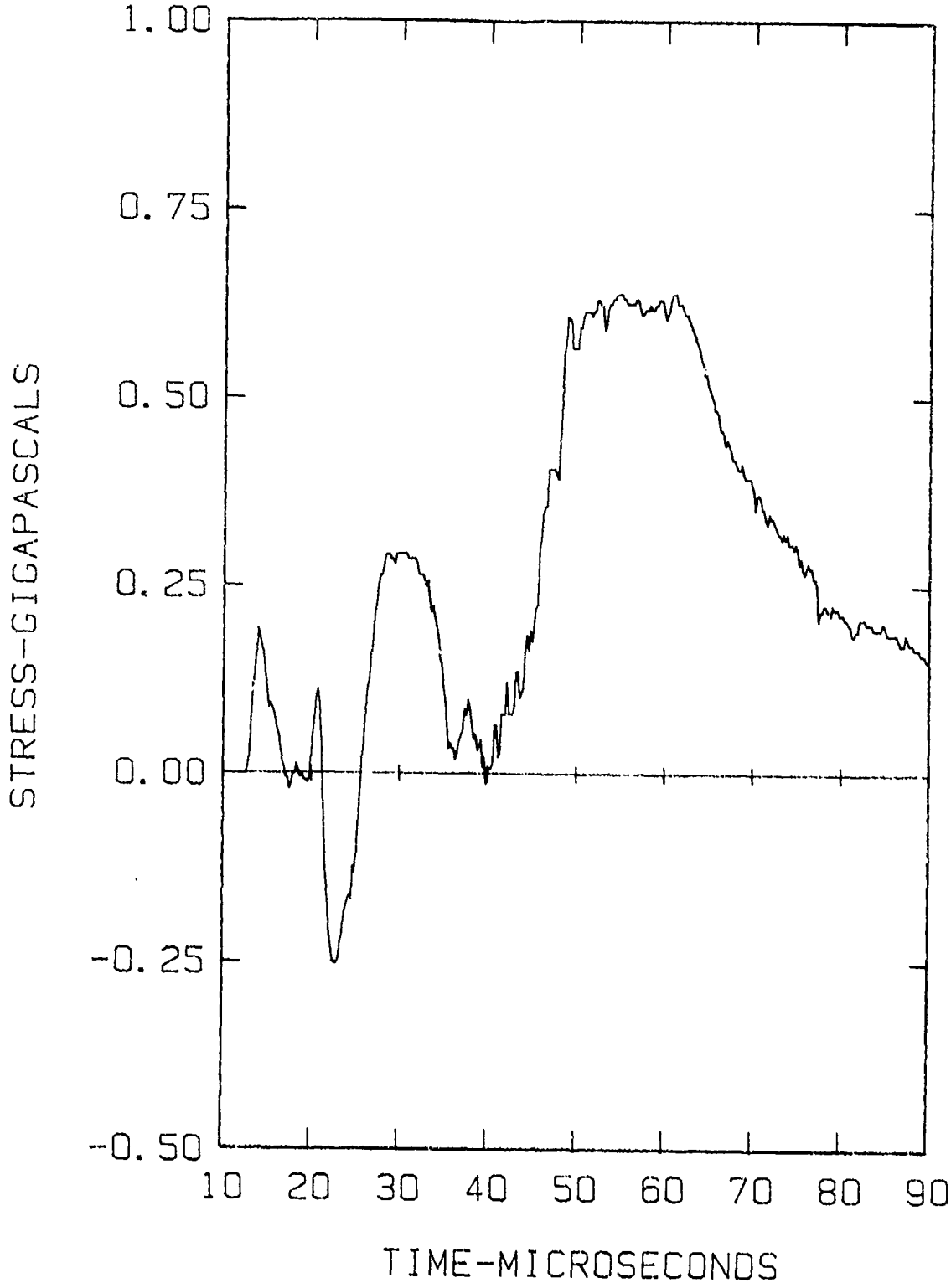

Figure 10. Stress Measuremont from Gage at 63.5 mm in Test No. 14

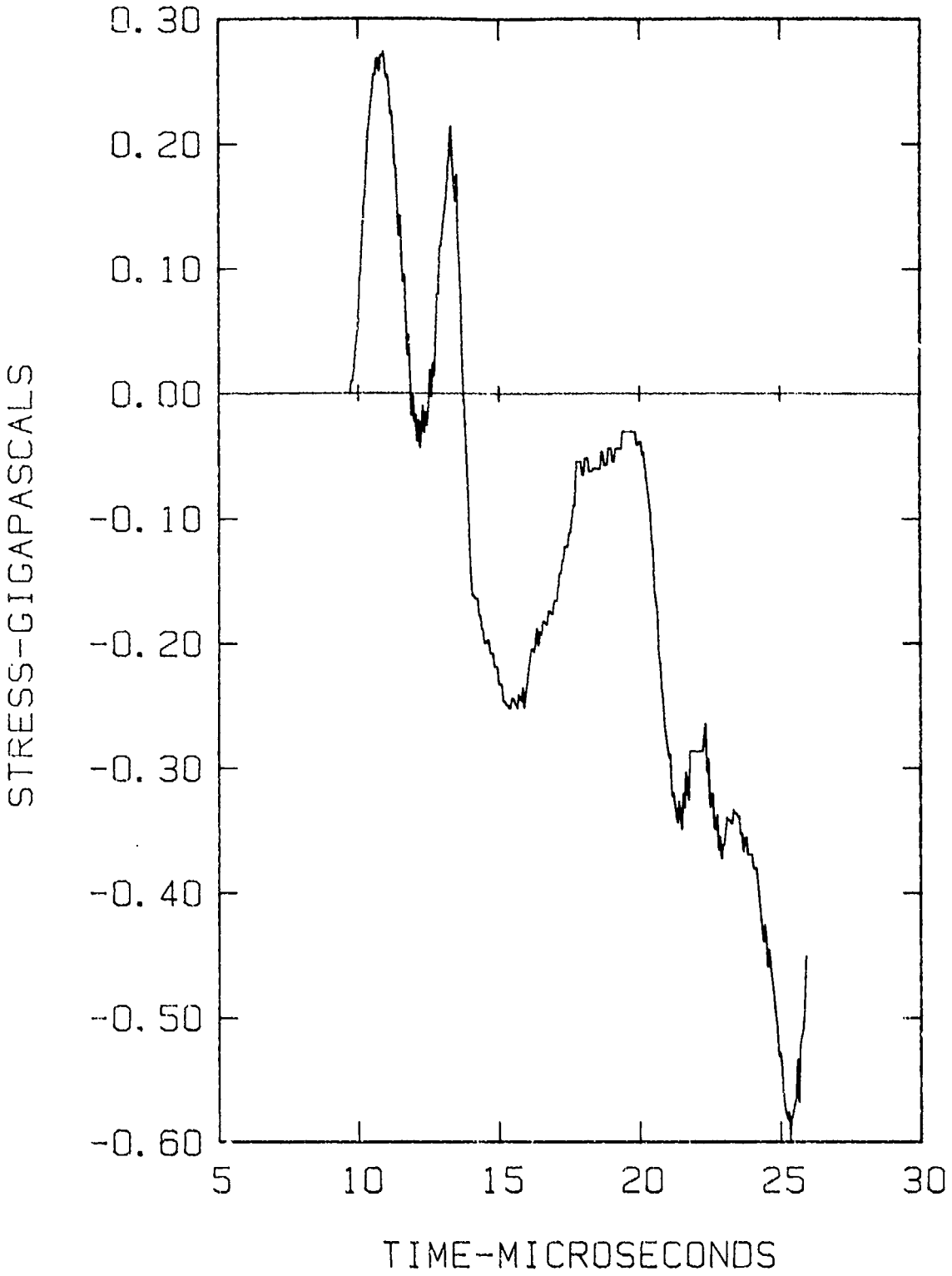

Figure 11. Stress Measurement from Gage at 44.45 mm in Test No. 15

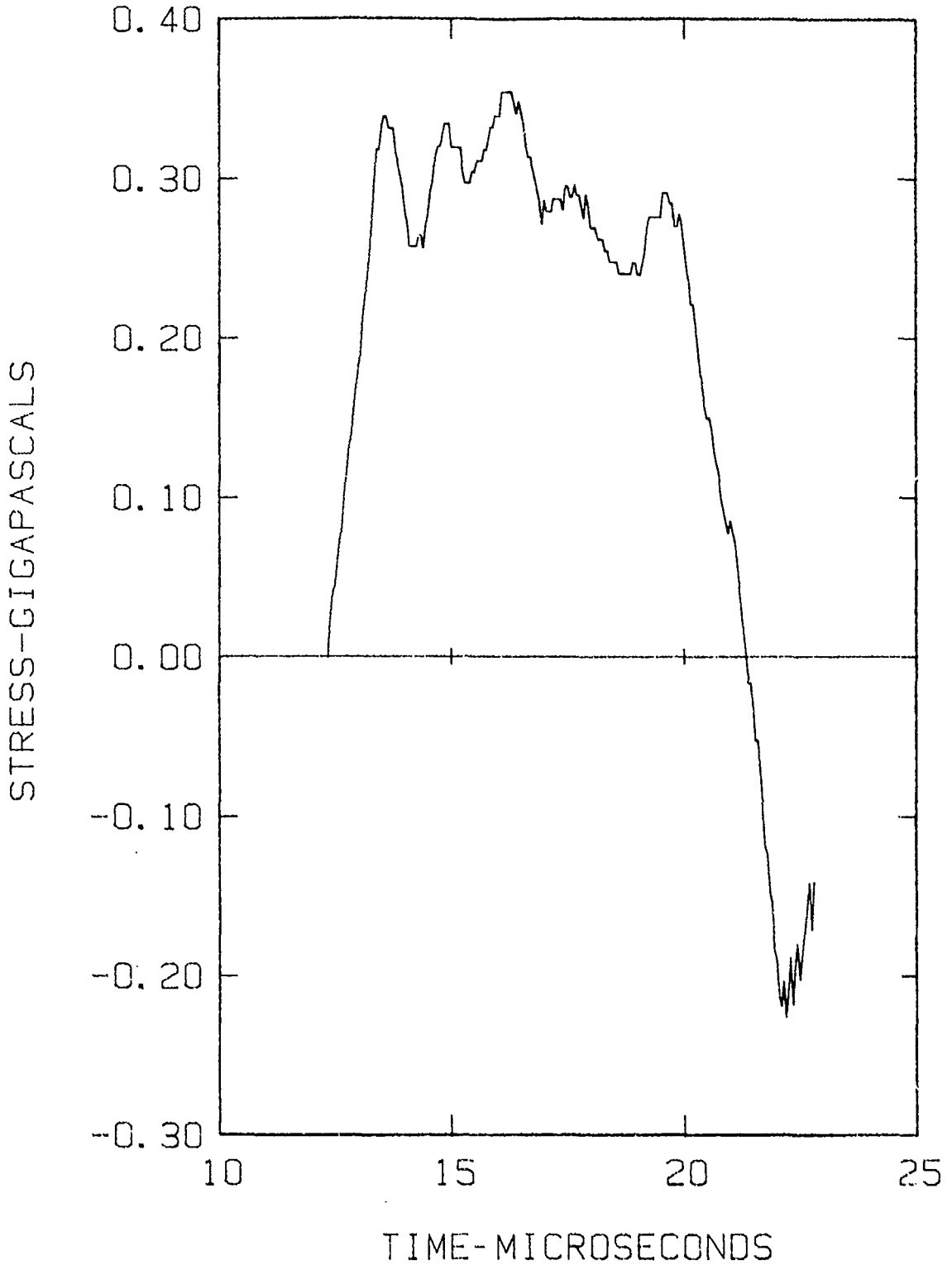

Figure 12. Stress Measurement from Gage at 63.5 mm in Test No. 15. Gage was not in slot.

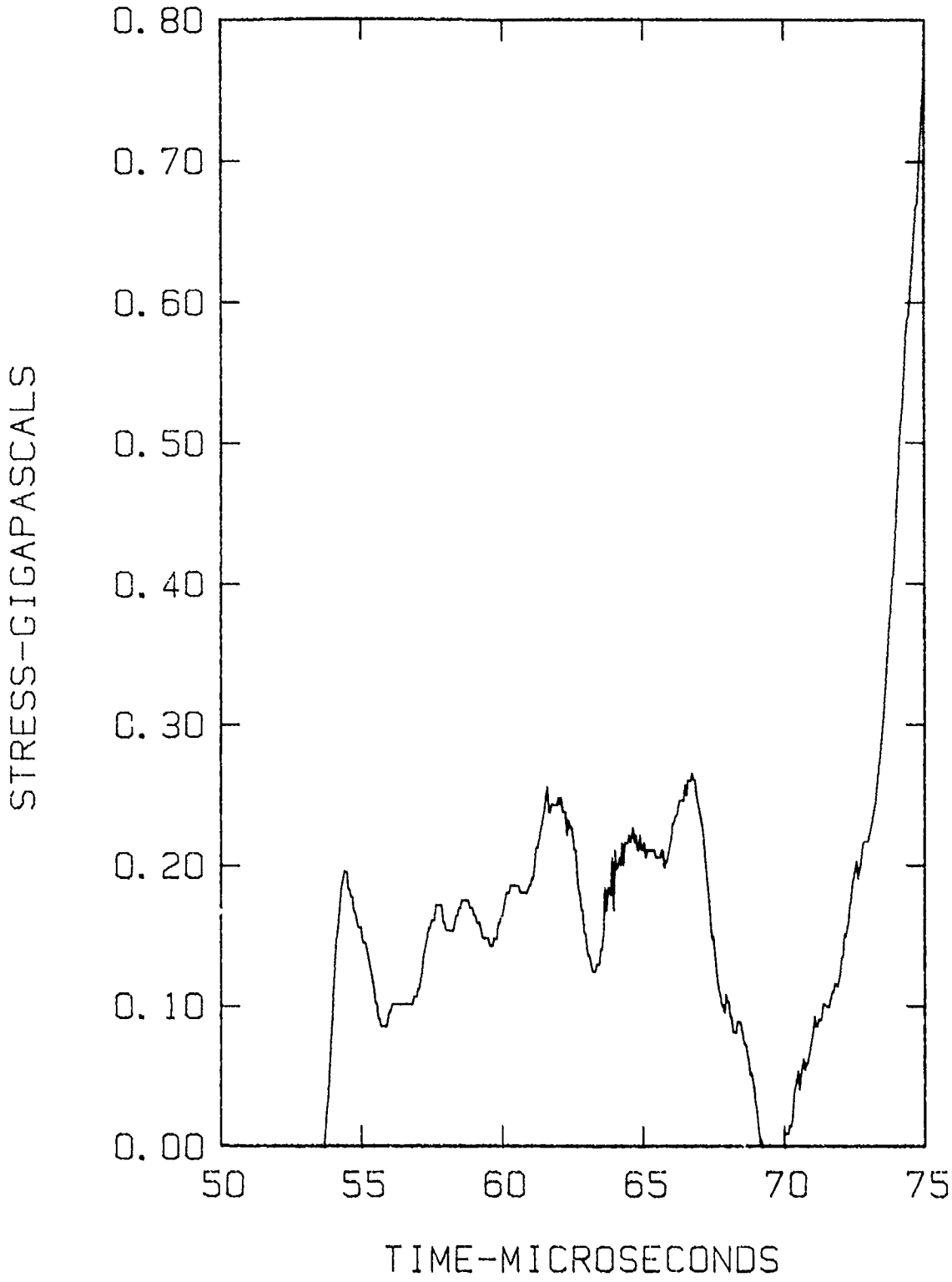

Figure 13. Stress Measurement from Test No. 16. Gage was not in slot.

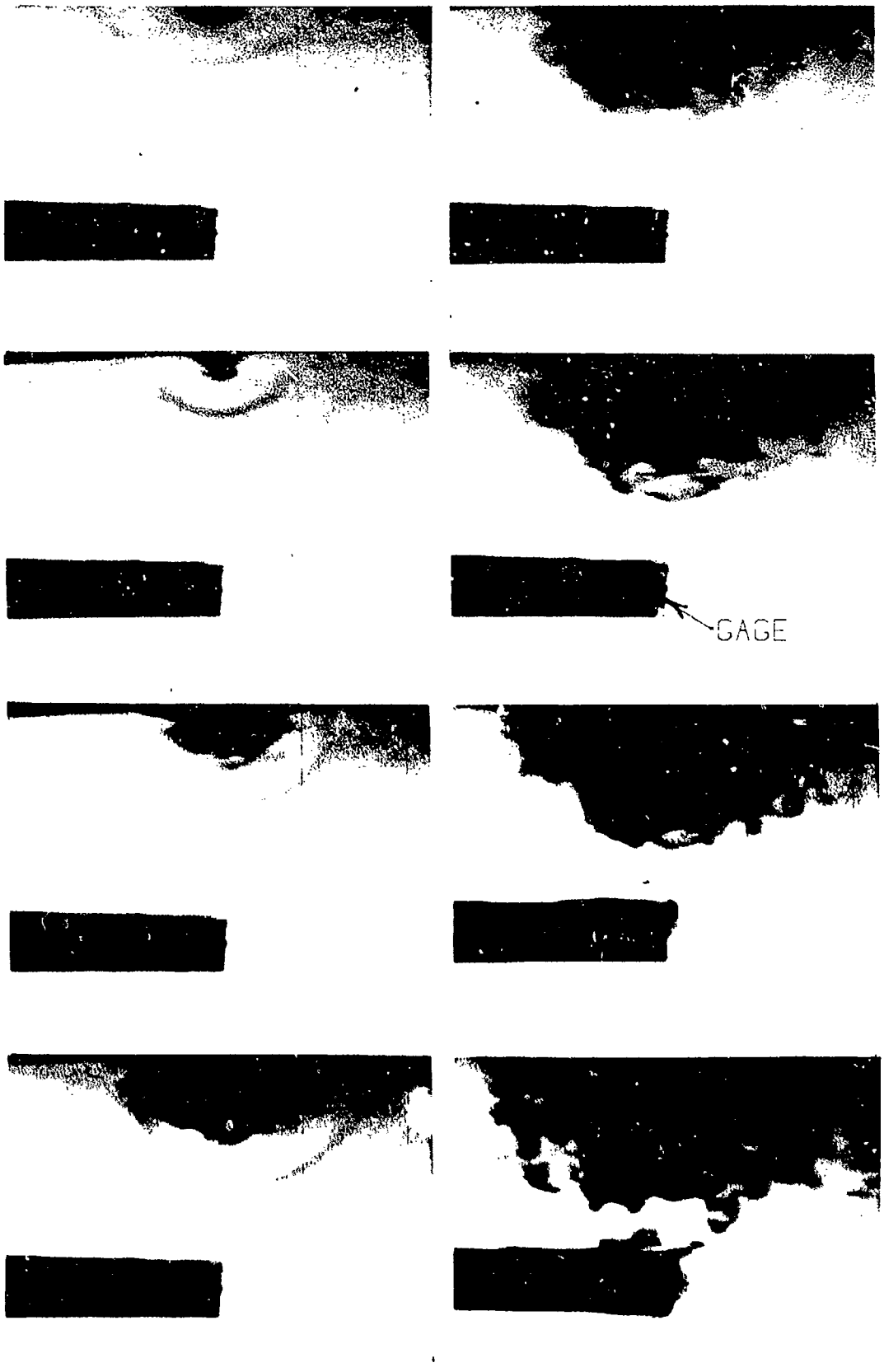

Figure 14. Framing Camera Frames from Test No. 8. Time between frames is 2 microseconds. The dark part of the gage slot is 16 mm wide.

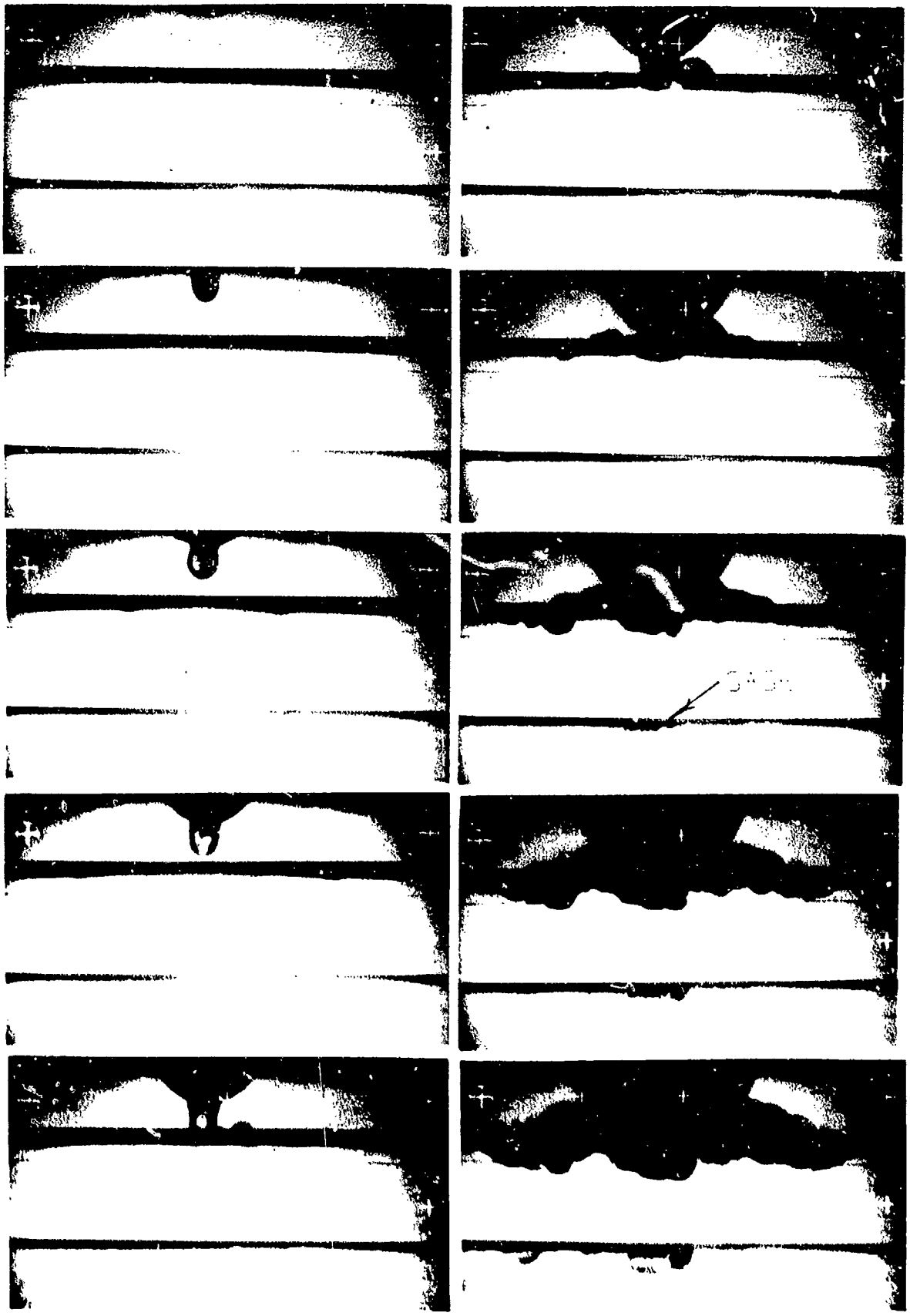

Figure 15. Framing Camera Frames from Test No. 10. Time between frames is 1.33 microseconds. Fiducial marks are spaced 25 mm apart.

jet impacted the cover plate. There was a delay of about 3 microseconds after shock arrival before cracking was seen at the gage. Data from the film in Figure 15 was used to calculate the shock velocity, the initial penetration velocity, and the glass fracture velocity. The measured values are:

Penetration Velocity = 2.57 km/s

Fracture Velocity = 2.10 km/s

Shock Velocity = 5.90 km/s.

The wave profiles determined with the stress gages were difficult to interpret when compared to the high speed framing camera photographs. For instance, at least two shock waves are evident in the photographs of the glass in Test No. 8 where the cover plate consisted of 25.4 mm of RHA and 25.4 mm of PMMA. The first wave was caused by the original jet impact at the RHA surface and the second (probably) by the impact of the jet reaching the PMMA-glass interface. In the steel, the shock velocity was higher than the penetration velocity, whereas, in the PMMA the opposite was true. The jet reached the glass interface approximately 2.2 microseconds after the shock and accounts for the photographic results. The stress profile also showed a two wave structure but the spacing was 7 microseconds. A cover plate of PMMA 50.8 mm thick was used in Test no. 10. The photographs show a double wave structure but in this case the second shock is much weaker than for Test No. 8. Compare Figures 14 and 15. In the PMMA, the penetration velocity was higher than the shock velocity, and the jet tip arrived at the PMMA-glass interface before the shock. The jet impact produced a shock in the glass after which the following shock in the PMMA entered the glass and caused the double wave structure of the photographs. The photographs of Test No. 8, Figure 14, also show a weak third shock which can be ascribed to the same causes.

The stress profiles of Figures 8 and 9 do not explicitly show these waves. This is probably due to the reasons stated earlier and in the case of Test No. 8 also due to the fact that the gage was loaded side-on and the stress waves took 0.8 microseconds to travel over the active gage length. Nevertheless, information on representative stress levels and times were obtained. Levels much higher than those measured were not in evidence and would have been detected. Lower levels would have been suspect around such an energetic process as shaped-charge jet penetration. It is believed that strain-compensated stress gages are essential in making this kind of measurement. Reliable measurements 3 to 4 microseconds after the arrival of the stress wave would have been impossible without their use.

V. CONCLUSIONS

The following conclusions were drawn from the experience gained in applying stress gage technology to the measurement of stress during shaped-charge jet penetration in glass, and from the combined photographic and stress results of this study.

First, the stress profiles measured were limited by both the mechanical and electrical response of the instrumentation. Electrical response could be most easily improved but would not materially enhance the measurements unless better packaging or other type of protection for the stress gages is devised.

Second, the stress measurements, with their shortcomings, were of sufficient quality to indicate stress levels in the immediate vicinity of a penetrating jet. It should be pointed out that the placement of the stress gages coincided with existing interfaces in the glass targets. The photographic results indicate that these interfaces influence the penetration by initiating cracking before penetration occurs. Insertion of foil stress gages in monolithic glass or ceramics would be impossible without creating interfaces for nucleation of fracture, thereby, influencing the penetration and the measurements.

As a corollary to the previous conclusion, and as stated earlier, strain-compensated stress gages are essential to satisfactory measurements in these kinds of materials.

Third, although higher stress levels than those measured in these experiments must be present at the jet-glass penetration interface, they will be difficult, if not impossible to measure with foil stress gages. Studying this interaction area in more suitable materials such as metals, where fracture does not constitute such a large part of the failure mechanisms, is possible with these gages. Future progress in measuring stress in glass or ceramics under shaped-charge attack will probably not come from foil stress gage technology. This statement is probably just as true for kinetic energy penetration in these materials.

Fourth, the information presented here can be used in analysis or design considerations for armor or anti-armor applications. The stress measurements can be used to verify analysis which can infer stress levels in inaccessible locations in a target. The photographic results determined some of the phenomenology of shaped-charge jet penetration in layered glass by identifying both the location and temporal history of the material failure.

REFERENCES

1. Allison, F. E., Defeat of Shaped Charge Weapons, Final Report, Contract No. DA-36-061-ORD-507, Carnegie Institute of Technology, April 1960.

2. Hauver, G. E., Melani, A., Franz, R. E. and Lawrence, W. Studies of Jet Penetration in Glass, Proceedings of AMC/DARPA Ceramic Composite Armor/Anti-Armor Program Review, 4-5 December 1984, Watertown MA.

3. Gupta, S. C. and Gupta, Y. M. Effect of Matrix Properties on the Piezoresistance Response of Ytterbium and Manganin Foils, Bulletin of the American Physical Society, Vol. 29, No. 4, 741, April 1984.

4. Rapacki, Jr., E. J., Instrumentation Techniques for Measuring Large, High Rate Strains with Foil Resistance Strain Gages, Ballistic Research Laboratory Technical Report ARBRL-TR-02573, August 1984.

5. Franz, R. E., The Measurement of Large Strains with Foil Resistance Strain Gages, Ballistic Research Laboratory Technical Report ARBRL-TR-02519, August 1983. ADA 133686.

6. Charest, J. A., Characterization of an Encapsulated 50-Ohm Manganin Foil Piezoresistive Gauge, Air Force Weapons Laboratory Report No. AFWL-TR-71-81, August 1972.

DISTRIBUTION LIST

No. of Copies	Organization
12	Administrator Defense Technical Info Center ATTN: DTIC-DDA Cameron Station Alexandria, VA 22304-6145
1	Deputy Assistant Secretary of the Army (R&D) Department of the Army Washington, DC 20310
1	HQDA DAMA-ARP-P, Dr. Watson Washington, DC 20310
1	HQDA DAMA-ART-M Washington, DC 20310
1	HQDA DAMA-MS Washington, DC 20310
1	Director US Army Ballistic Missile Defense Systems Office 1320 Wilson Boulevard Arlington, VA 22209
1	Commander US Army War College ATTN: Lib Carlisle Barraacks, PA 17013
1	Commander US Army Command and General Staff College ATTN: Archives Fort Leavenworth, KS 66027
1	Commander US Army Materiel Command ATTN: AMCDRA-ST 5001 Eisenhower Avenue Alexandria, VA 22333-0001
1	Commander US Army Armament, Munitions and Chemical Command ATTN: SMCAR-ESP-L Rock Island, IL 61299
1	Commander Armament R&D Center US Army AMCCOM ATTN: SMCAR-TDC Dover, NJ 07801
1	Commander Armament R&D Center US Army AMCCOM ATTN: SMCAR-TSS Dover, NJ 07801
1	Director Benet Weapons Laboratory Armament R&D Center US Army AMCCOM ATTN: SMCAR-LCB-TL Watervliet, NY 12189
1	Commander US Army Aviation Research and Development Command ATTN: AMSAV-E 4300 Goodfellow Boulevard St. Louis, MO 63120
1	Director US Army Air Mobility Research and Development Command Ames Research Center Moffett Field, CA 94035
1	Commander US Army Communications - Electronics Command ATTN: AMSEL-ED Fort Monmouth, NJ 07703-5301

DISTRIBUTION LIST

No. of Copies	Organization
1	Commander ERADCOM Technical Library ATTN: DELSD-L (Reports Section) Fort Monmouth, NJ 07703-5301
1	Commander US Army Development and Employment Agency ATTN: MODE-TED-SAB Fort Lewis, WA 98433
1	Commander US Army Harry Diamond Laboratory ATTN: DELHD-TA-L 2800 Powder Mill Road Adelphi, MD 20783
1	Commander MICOM Research, Development and Engineering Center ATTN: AMSMI-RD Redstone Arsenal, AL 35898
1	Director Missile and Space Intelligence Center ATTN: AIAMS-YDL Redstone Arsenal, AL 35898-5500
1	Commander US Army Ballistic Missile Defense Systems Command ATTN: SENSC, Mr. Davidson P. O. Box 1500 Huntsville, AL 35804
3	Director BMD Advanced Technology Center ATTN: ATC-T, M. Capps ATC-M, S. Brockway ATC-RN, P. Boyd P.O. Box 1500, West Station Huntsville, AL 35807
2	Commander US Army Mobility Equipment Research & Development Command ATTN: DRDME-WC DRSME-RZT Fort Belvoir, VA 22060
1	Commander US Army Natick Research and Development Center ATTN: DRXRE, Dr. D. Sieling Natick, MA 01762
1	Commander US Army Tank Automotive Command ATTN: AMSTA-TSL Warren, MI 48397-5000
1	Commander US Army Electronics Proving Ground ATTN: Tech Lib Fort Huachuca, AZ 85613
3	Commander US Army Materials and Mechanics Research Center ATTN: AMXMR-T, J. Mescall AMXMR-T, R. Shea AMXMR-H, S.C. Chou Watertown, MA 02172
1	Commander US Army Research Office P. O. Box 12211 Research Triangle Park, NC 27709
1	Director US Army TRADOC Systems Analysis Activity ATTN: ATAA-SL White Sands Missile Range, 88002

DISTRIBUTION LIST

No. of Copies	Organization
1	Commandant US Army Infantry School ATTN: ATSH-CD-CSO-OR Fort Benning, GA 31905
2	Office of Naval Research Department of the Navy ATTN: Code 402 Washington, DC 20360
1	Commander Naval Surface Weapons Center ATTN: Code Gr-9, Dr. W. Soper Dahlgren, VA 22448
1	Commander and Director US Naval Electronics Laboratory ATTN: Lib San Diego, CA 92152
1	Air Force Armament Laboratory ATTN: AFATL/DLODL Eglin AFB, FL 32542-5000
1	AFWL/SUL Kirtland AFB, nM 87117
1	New Mexico Institute of Mining and Technology Socorro, NM 87801
2	SRI International ATTN: Dr. D. Curran Dr. L. Seaman 333 Ravenswood Avenue Menlo Park, CA 94025
10	Central Intelligence Agency Office of Central Reference Dissemination Branch Room GE-47 HQS Washington, D.C. 20502
2	Southwest Research Institute Department of Mechanical Sciences ATTN: Dr. U. Kindholm Dr. W. Baker 8500 Culebra Road San Antonio, TX 78228
1	The Johns Hopkins University ATTN: Prof. W. Sharpe 34th and Charles Streets Baltimore, MD 21218
1	University of Denver Denver Research Institute 2390 S. University Boulevard Denver, CO 80210

Aberdeen Proving Ground

Dir, USAMSAA
ATTN: AMXSY-D
AMXSY-MP, H. Cohen
Cdr, USATECOM
ATTN: AMSTE-TO-F
Cdr, CRDC, AMCCOM
ATTN: SMCCR-RSP-A
SMCCR-MU
SMCCR-SPS-IL

USER EVALUATION SHEET/CHANGE OF ADDRESS

This Laboratory undertakes a continuing effort to improve the quality of the reports it publishes. Your comments/answers to the items/questions below will aid us in our efforts.

1. BRL Report Number _____ Date of Report _____

2. Date Report Received _____

3. Does this report satisfy a need? (Comment on purpose, related project, or other area of interest for which the report will be used.) _____

_____

_____

4. How specifically, is the report being used? (Information source, design data, procedure, source of ideas, etc.) _____

_____

_____

5. Has the information in this report led to any quantitative savings as far as man-hours or dollars saved, operating costs avoided or efficiencies achieved, etc? If so, please elaborate. _____

_____

_____

6. General Comments. What do you think should be changed to improve future reports? (Indicate changes to organization, technical content, format, etc.)

_____

_____

_____

CURRENT ADDRESS

_____
Name

_____
Organization

_____
Address

_____
City, State, Zip

7. If indicating a Change of Address or Address Correction, please provide the New or Correct Address in Block 6 above and the Old or Incorrect address below.

OLD ADDRESS

_____
Name

_____
Organization

_____
Address

_____
City, State, Zip

(Remove this sheet along the perforation, fold as indicated, staple or tape closed, and mail.)

FOLD HERE

Director
U.S. Army Ballistic Research Laboratory
ATTN: SLCBR-DD-T
Aberdeen Proving Ground, MD 21005-5066

NO POSTAGE
NECESSARY
IF MAILED
IN THE
UNITED STATES

OFFICIAL BUSINESS
PENALTY FOR PRIVATE USE, $300

BUSINESS REPLY MAIL
FIRST CLASS PERMIT NO 12062 WASHINGTON, DC
POSTAGE WILL BE PAID BY DEPARTMENT OF THE ARMY

Director
U.S. Army Ballistic Research Laboratory
ATTN: SLCBR-DD-T
Aberdeen Proving Ground, MD 21005-9989

FOLD HERE